



ISSN: 2617-6548

URL: [www.ijirss.com](http://www.ijirss.com)



## Development of an adaptive two-phalanx grip model for robotic manipulators

 Karassaeyv Bairon<sup>1,4</sup>,  Makhanbetova Sandugash<sup>2\*</sup>,  Kunelbayev Murat<sup>1,3</sup>,  Temirbekov Yerbol<sup>1,4</sup>,  
 Akhmetzhanov Maksat<sup>1</sup>

<sup>1</sup>*Al-Farabi Kazakh National University, Almaty, Kazakhstan.*

<sup>2</sup>*Kazakh National Women's Teacher Training University, Almaty, Kazakhstan.*

<sup>3</sup>*Institute of Information and Computational Technologies CS MES RK, Al-Farabi Kazakh National University, Almaty, Kazakhstan.*

<sup>4</sup>*Institute of Mechanics and Engineering Science named after U.A. Dzholdasbekova, Almaty, Kazakhstan.*

Corresponding Author: Makhanbetova Sandugash (Email: [sandu.ms@mail.ru](mailto:sandu.ms@mail.ru))

### Abstract

The purpose of this work is to study the problem of uniform grip at the points of contact of a round or spherical object (fruits and vegetables) with the grip. The research methodology uses pressure sensors mounted on the “fingers” of the handle. At a certain force value in the contact zone, the “fingers” of the handle stop. The grip must create equal forces at the points of contact of all “fingers” for an even grip. To explore these issues, phalangeal graspers adapting to the fetal surface are analyzed here. The flat model shows the general patterns of the relationship between the forces of the “fingers” of the grip and the round object to be grasped. The flat model shows the general patterns of the relationship between the forces of the “fingers” of the grip and the round object to be grasped. We examined the 3D model of this gripper and calculated the parameters of the 3D model. Conclusions and practical consequences are the values of stresses and elastic displacements at the points of the contact lines of the teeth of the 3D models of the gripper and the object being grabbed. The distribution of forces on a flat diagram and the values of von Mises stresses in the 3D model demonstrate a certain similarity in the uniformity of distribution of these parameters. Color scales with the values of the corresponding parameters are also presented; the calculation was carried out using the finite element modeling method in inventor.

**Keywords:** 3D modeling, Adaptive grip, Pressure sensor, Robotic manipulators, The range of force measurement, Two phalanges.

**DOI:** 10.53894/ijirss.v7i2.2856

**Funding:** This study received no specific financial support.

**History: Received:** 28 September 2023/**Revised:** 11 December 2023/**Accepted:** 16 February 2024/**Published:** 7 March 2024

**Copyright:** © 2024 by the authors. This article is an open access article distributed under the terms and conditions of the Creative Commons Attribution (CC BY) license (<https://creativecommons.org/licenses/by/4.0/>).

**Authors' Contributions:** All authors contributed equally to the conception and design of the study. All authors have read and agreed to the published version of the manuscript.

**Competing Interests:** The authors declare that they have no competing interests.

**Transparency:** The authors confirm that the manuscript is an honest, accurate, and transparent account of the study; that no vital features of the study have been omitted; and that any discrepancies from the study as planned have been explained. This study followed all ethical practices during writing.

**Institutional Review Board Statement:** Not applicable.

**Publisher:** Innovative Research Publishing

## 1. Introduction

This article by [Ren, et al. \[1\]](#) presents the construction of a new hand with low mobility with highly integrated modular finger blocks that can be freely reconfigured in terms of the position of the fingers and their number, taking into account the need for manipulation in various applications. In the article by [Ryu, et al. \[2\]](#) a prosthetic hand was created for people with amputated fingers and metacarpal bone. Designing the drive vertically between the finger modules and the mounting part into which the electrical parts integrated results in the useful arrangement. In this study, all the scaffolds used in the proposed prosthetic brush were made of nylon by multi-jet fusion multidimensional printing method. In [Wahit, et al. \[3\]](#) a robotic arm mechanism with improved data (a coupling mechanism with four rods) was proposed, which overcomes the disadvantage of using a cable-driven mechanism, which leads to the least structural force and an incorrect range of movement. Robotic weapons have an endless range of uses. There are many types of robotic arms, some of which are used to manufacture robots, and some of them, prosthetic arms, are used to attach to the human body to replace a person's lost arm with an amputated limb. In patients with upper limb amputations, hand prostheses allow not only to cosmetically replace the lost limb, but also to restore certain functions of the hand. In [Wu, et al. \[4\]](#); [Liow, et al. \[5\]](#); [Van and Van \[6\]](#); [Dang, et al. \[7\]](#); [Belter, et al. \[8\]](#) and [Zhang, et al. \[9\]](#) they developed a robotic hand with five fingers, each of which has two degrees of freedom. In their paper, [Li, et al. \[10\]](#) came up with a robotic hand with slightly activated fingers, driven by three levers. [Liu, et al. \[11\]](#) proposed to use an incomplete two-finger grip to grasp unknown objects. [Reis, et al. \[12\]](#) recommended using a three-finger robotic hand based on a combination of flexible tendons for adaptive gripping. In the paper [Wattanasiri, et al. \[13\]](#) a prosthetic hand was proposed that is capable of performing several gripping variations using only one actuator, made on a lever actuator. However, the hand lacks the ability to perceive. [Cordella, et al. \[14\]](#) created a bionic pen with sensing capability similar to real-time sliding object detection. However, the finger mechanism appears larger due to the integration of the maximum number of sensitive components. In article [Palli, et al. \[15\]](#) an innovative mechanized hand was studied, which has absolutely all the degrees of freedom of the human hand. Thanks to the maximum number of degrees of freedom, it is more problematic to control. Thus, dexterous hands are either unimaginably complex in structure or lack the significant functions for dexterous hands. From the point of view of information perception, scientists are most interested in the effect of data capture on objects sliding along the hand. In [Wu, et al. \[16\]](#) the finger was examined using an integrated automatic sensor, which is prepared to simultaneously measure the grip force and the contact position when the hand picks up an object. Based on the principle of finding surface structure, [Venter and Mazid \[17\]](#) built a tactile sensor to detect objects sliding in a robot's hand. The paper by [Luberto, et al. \[18\]](#) recommended an adaptive grasping strategy based on object location estimation using provided point clouds. [Park, et al. \[19\]](#) came up with the idea of adjusting finger gripping motion based on soft sensors. A process capture mechanism using a camera was used to test the performance. In [Othman, et al. \[20\]](#) a critical micro potentiometer was used to measure and control finger flexion. Versatility appears to be a significant feature of prosthetic hands. The human hand has 21 degrees of freedom and a unique structure. It is very difficult to design a bionic prosthetic arm that has the same degrees of freedom as a human arm. In practice, a prosthetic hand requires a sufficient number of machined components, especially in order to be able to perform gestures that are especially frequently used in everyday life. The ability to perceive information appears to be another necessary feature of a prosthetic hand [8, 21, 22]. For fingers based on a single joint, there is no need to place angle sensors in the fingers since the angles of an arbitrary combination can be calculated from the proportions between the joints. However, tilt sensors are important for an adaptive finger with several degrees of freedom. Based on available research, most prosthetic arms do not have joint-angle sensors due to limited design control. This does not guarantee that the control structure will accept the position of grasping an object with an unrealistic hand.

The tendency to increase our physical, aesthetic, and multifunctional lifestyle has forced people to engage in innovative solutions that help patients exposed to incomplete or complete loss of body parts [23, 24]. The engineering shift has presented significant importance in the development of prostheses. These devices are designed to replace organs and body parts, allowing the patient to half or completely adjust the functional abilities of the body [25]. Prostheses may have aesthetic or functional features; in this case, aesthetic prostheses naturally supply near-term performance or do not have it at all and are designed to prompt the confused limb of the owner, ignoring its functionality. On the other hand, functional prostheses are oriented towards recreating the functional abilities of a confused limb [26]. Currently, due to scientific and technological progress in the field of miniaturization, prostheses have evolved from systems powered by the body [27] to mechatronic devices [28] capable of taking the patient's action and influencing him [Singh \[29\]](#). In [Pollayil, et al. \[30\]](#) a self-adjusting gripping routine has been developed that benefits from synchronized finger and wrist processes, which can increase the possibility of effective gripping and reduce the slipping of the object during the closing of the hands. The paper by [Hussain, et al. \[31\]](#) explores several aspects integrated with the design, modeling, prototyping, and testing of soft-hard tendon grippers. The design and development of a two-finger handle were presented as a sample to demonstrate the application scenario of a mathematical model based on the concept of screws. The following is a mathematical formulation based on the concept of screws to model gripper dynamics. The proposed formulation appears to be an extension of the previously presented model to include the dynamics of a mechanical system. While keeping the grip's kinematic structure the same and changing how it deforms when not in use, this type of grip can have a lot of different properties. For example, it can have different fingertip processes, which are the same thing as different ellipsoids of finger tip stiffness. Determined the primary characteristics of the gripper in terms of payload and maximum horizontal resistance, and tested the gripping capabilities for grasping objects of various shapes and weights. As the use of robots has expanded, flexible robotic grippers have been developed to handle objects of varying sizes, shapes, materials, and surface properties. However, normal grips lack the rigidity and stability of rigid grips due to their inherent design limitations. The article [Ji, et al. \[32\]](#) recommended a mixed plastic robotic gripping mechanism using both a solid link and a plastic vertebra-type mechanism to improve the

rigidity and stability of the grip. The recommended mechanism will be able to reasonably implement a power grip due to the methodical movement of a solid link and an elastic mechanism. In robotic urological surgery, the assistant usually uses laparoscopic forceps to move organizations outside of the surgical workplace, but the effectiveness of the support is not too great. In the study by Hashira, et al. [33] a three-dimensional humanoid paw with some independence steps was created, as well as a folding device that would allow it to be implemented through a small cross-section in order to increase the performance of the support offered along with the organs. In recent years, the effectiveness of robotic garbage collection has attracted increasing respect due to the development of more and more absolute cameras and machine vision systems, collective and industrial robots, as well as complex robotic grips. In the process of verification sorting, a huge variety of objects in terms of shape, weight, and surface calls for complicated conclusions for a reliable selection of objects. A difficult element of robotic garbage collection is contained in the correct finding of object collection points. The article by Bencak, et al. [34] presents a simulation model based on Matrix Laboratory MATLAB for a robotic evaluation of the capture point for a 2-F robotic capture. It consists of a mechanical model erected in ADAMS/View, a MATLAB/Simulink power controller, several additional functions, and a graphical user interface created in MATLAB/App Designer.

The purpose of this work is to solve the problem of uniform capture at the points of contact of a round or spherical object (fruits and vegetables) with the capture.

## 2. Methodology

The methodology of this study is the development of an adaptive model of capture by two phalanges using 3D modeling.

Figures 1a, and b present a method of creating cheap verbal work printed on a 3D printer. The robot's height is approximately 170 cm, corresponding to a healthy person's typical height. This robot consists of two parts: the front of the verbal robot printed on a 3D printer, the back of the articulated robot printed on a 3D printer, and the mobile base. The portable base is made of iron and has to be moved by three engines with a power of 1000 watts. For a verbal work of natural size with the highest mobility, it is infinitely economical.

As shown in Table 1, the robot has 27 motors, 25 servos with a variety of overloads, and 3 main motors specially prepared for 24V electrical control. A 16Ah lithium battery is present, placed in a movable base, and guarantees all the galvanic operation of the robot.

**Table 1.**  
Degrees of freedom of verbal robot.

Part	Degree of freedom	Motors
Right and left hand	30	10
Wrist	2	2
Elbow	2	2
Shoulder	6	6
Head	3	3
Waist	1	2
Mobile base	6	3

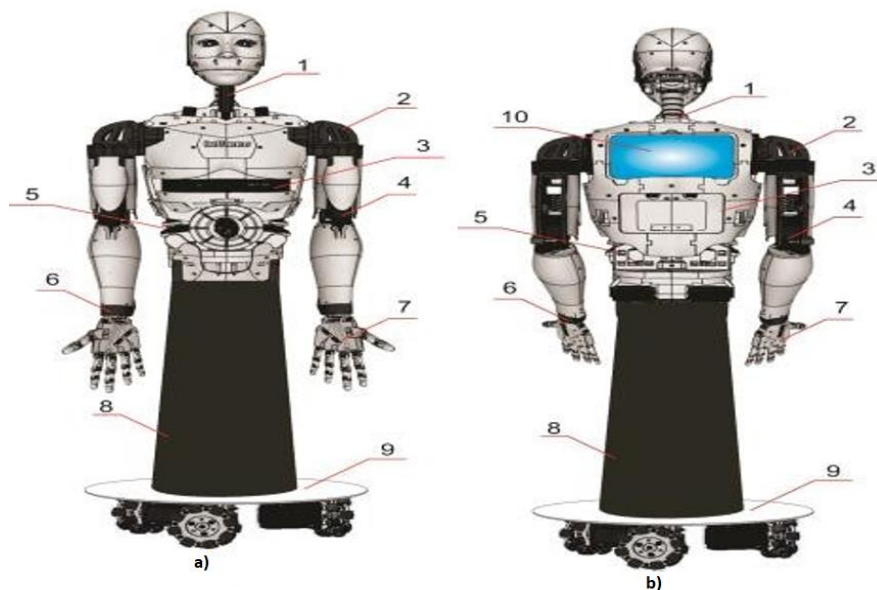


**Figure 1.**  
a) 3D printed front side of the verbal robot; b) 3D printed back side of the verbal robot.

Advantages of wheeled robots: they are faster, more stable, freely controllable, more efficient, and can provide a huge necessary load during implementation. A large degree of freedom allows fruitful movement diagonally, to the right, to the left, and forward, and backward.

The verbal robot consists of 1 head, 2-shoulder, 3-face detection devices, 4-elbow, 5-trunk, 6-hand, 7-forearms, 8-platform for controlling the entire system, 9-omnidirectional mobile platforms, 10-touch screens.

The mobile platform includes three all-usable wheels, each of which is placed at a distance of 120 degrees from each other so that the robot remains stationary, and three distinctive engine wheels so that the robot moves.

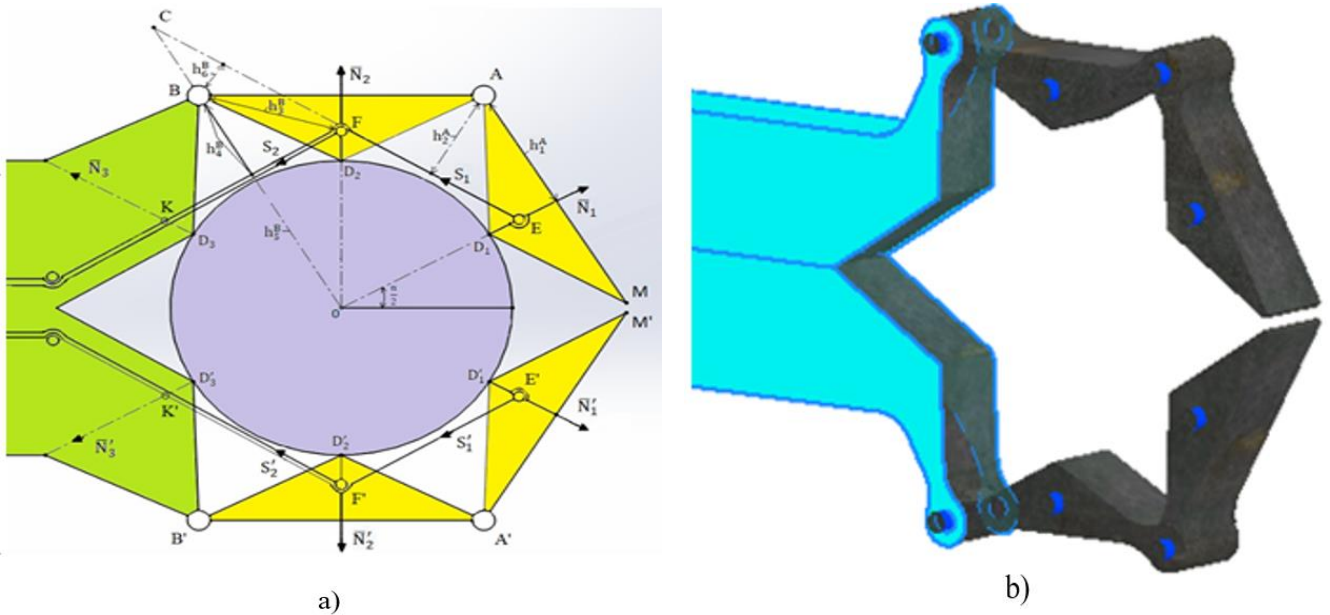
Figure 2 shows a robot arm printed on a 3D printer with a brush.



Figure 2.  
Robot arm.

It is called adaptive because each of the fingers has two phalanges connected by hinges and, accordingly, two degrees of freedom. And if the surface of the captured body does not differ much from a circle or a sphere, then due to the available degrees of freedom, the phalanges are adapted to this surface. The phalanges of the grasp are triangular in profile and symmetrical about the radial line (Figure 3a). On a circle of radius  $R_2$ , there are hinges A, B, A', B', and points M and M'. The radius of the section circle of the object to be grasped is  $R_1$ , and the relation  $R_2 > R_1$  is fulfilled. Flexible traction element 1 (GTE-1) is fixed at points E and E', from point E, it passes through points F and K and then goes to drive-1; from point E' it passes through points F' and K' and then goes also to the drive-1. Flexible traction element 2 (GTE-2) is fixed at points F and F', from point F it passes through point K and then also goes to drive-2; from point F', it passes through point K' and then also goes to drive-2. At points D1, D2, and D3, where the teeth of the gripper are located, GTE-1 and GTE-2 should be as close as possible to the circle of radius  $R_1$  to create a greater force in the teeth. From the condition that GTE-1 and GTE-2 do not touch this circle of the section of a cylindrical part, we have  $(R_1 + a) \cos(\alpha / 2) > R_1$ , or  $a > R_1 / \cos(\alpha / 2) - R_1$ , where  $a = ED_1 = E'D'_1 = FD_2 = F'D'_2$  and  $\alpha$  is the central angle (Figure 1a). Let  $\alpha = 60^\circ$ , then the grip of the grasped object with the "fingers" together with the fragment of the handle will be equal to the circumference. GTE-1 and GTE-2 should be as close as possible to a circle of radius  $R_1$  to create a greater force in the teeth. From the condition that GTE-1 and GTE-2 do not touch this circle of the section of a cylindrical part, we have  $(R_1 + a) \cos(\alpha / 2) > R_1$ , or  $a > R_1 / \cos(\alpha / 2) - R_1$ , where  $a = ED_1 = E'D'_1 = FD_2 = F'D'_2$  and  $\alpha$  is the central angle (Figure 3a). Let  $\alpha = 60^\circ$ , then the grip of the grasped object with the "fingers" together with the fragment of the handle will be equal to the circumference. GTE-1 and GTE-2 should be as close as possible to a circle of radius  $R_1$  to create a greater force in the teeth. From the condition that GTE-1 and GTE-2 do not touch this circle of the section of a cylindrical part, we have  $(R_1 + a) \cos(\alpha / 2) > R_1$ , or  $a > R_1 / \cos(\alpha / 2) - R_1$ , where  $a = ED_1 = E'D'_1 = FD_2 = F'D'_2$  and  $\alpha$  is the central angle (Figure 3a). Let  $\alpha = 60^\circ$ , then the grip of the grasped object with the "fingers" together with the fragment of the handle will be equal to the circumference.  $D'_1 D'_2 D'_3 \hat{o}$ .

Let's find the internal force that arises in the "tooth" 1 (point). From the condition of equilibrium of the moments of forces  $N_1 D_1 \sum M_{Ai} = 0$  (Figure 3a),  $N_1 = \frac{S_1 \cdot h_2^A}{h_1^A}$  where is the shoulder of the moment of effort; shoulder of the moment of effort  $h_1^A = R_2 \sin\left(\frac{\alpha}{2}\right) \bar{N}_1 h_2^A = R_2 - (R_1 + a) \cos\left(\frac{\alpha}{2}\right) \bar{S}_1$  - external force from GTE-1.



**Figure 3.** Flat diagram and 3D-model of a biphallangeal grasp.

Let's find the internal force generated in tooth 2 (point D2). Let's consider the condition of equilibrium of moments of force (Figure 3a). From GTE-1, attached at point E, two reactions of equal magnitude appear at point F. They are directed: one from F to E, the second from F to K. Their sum is equal in absolute value and directed from point F to point O. This force creates a moment relative to point B, pressing phalanx 2 to the object of grasping. From the equilibrium condition, we have:

$$\bar{N}_2 \sum M_{Bi} = 0 \bar{S}_1 S_F = 2 S_1 \cdot \sin\left(\frac{\alpha}{2}\right) \quad (1)$$

$$N_2 h_3^B - S_2 h_4^B + S_1 h_6^B + N_1 h_5^B - S_F h_3^B = 0 \quad (2)$$

Where  $S_2$  - external effort from GTE-2.

$$h_3^B = h_1^A h_4^B h_2^A h_5^B = R_2 \sin\left(3 \frac{\alpha}{2}\right) \bar{N}_1 \quad (3)$$

Let's find - the shoulder of the moment from the effort  $h_6^B \bar{S}_1$  relative to point B. Find the coordinates of points E, F, C:

$$X_E = (R_1 + a) \cos\left(\frac{\alpha}{2}\right), Y_E = (R_1 + a) \sin\left(\frac{\alpha}{2}\right) \quad (4)$$

$$X_F = 0, Y_F = R_2 - (R_1 + a) \sin\left(3 \frac{\alpha}{2}\right), X_C = Y_C \cdot \frac{X_B}{Y_B}, Y_C = \frac{Y_F X_E}{X_E - X_B Y_E + X_B Y_F} \quad (5)$$

$$\angle OCE = 180^\circ - 90^\circ - 2 \frac{\alpha}{2} = 30^\circ \dots$$

Length BC =. In this case, the force is equal to:  $Y_C - R_2$ , then  $h_6^B = BC \sin(\angle OCE) \bar{N}_2$

$$N_2 = \frac{1}{h_3^B} (S_2 h_4^B - S_1 h_6^B - N_1 h_5^B + S_F h_3^B) \quad (6)$$

Force N1 should be equal in magnitude to the force in tooth 1 for uniform compression of the object, that is,  $N_2 = N_1 \dots$  Their directions are normal to the surface of the object at the points of their application. In a tooth lying on a handle pivotally connected to the nearest phalanx, from the condition of balance of efforts for the entire object of grasping and symmetry about point O, we have:  $N_3 = N_1$ . All these reactions are directed along the normals to the corresponding points

of the setting object (to the circle of radius R1). Then, from the vector condition of balance of efforts and symmetry of the gripper relative to the longitudinal axis, we have:

$$N1' = N1, N2' = N2, \text{ and } N3' = N3.D_3$$

Thus, we have obtained relations for static forces in a flat model of a two-finger, two-phalanx grip. Let us take as a model example the parameters of the flat circuit: R1 = 60 mm, R2 = 100 mm, α = 60°, and d = 15 mm. Table 1 and Figure 2 show the dependences of the calculated reactions N1, N2, N3, N1', N2', and N3' on the set values S1 and S2 on the drives transmitted by GTE-1 and GTE-2.

Table 2 presents the values of forces S1, S2, and reactions N1, N2, N3, N1', N2', N3'.

**Table 2.**  
Values of forces S1, S2 and reactions N1, N2, N3, N1', N2', N3'.

S1	S2	N1 = N1'	N2 = N2'	N3 = N3'
One hundred	Twenty	70,09	71,47	70,09
200	37	140,19	140,84	140,19
300	54	210,28	210,21	210,28
400	71	280,38	279,58	280,38
500	89	350,48	349,65	350,48

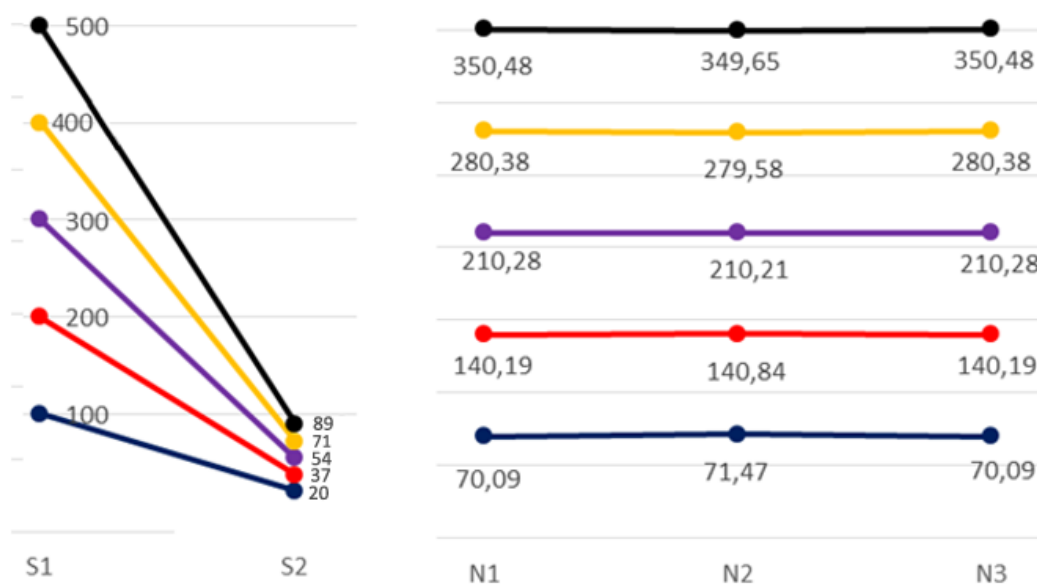


**Figure 4.**  
Diagrams of forces S1, S2 and reactions N1, N2, N3, N1', N2', N3'.

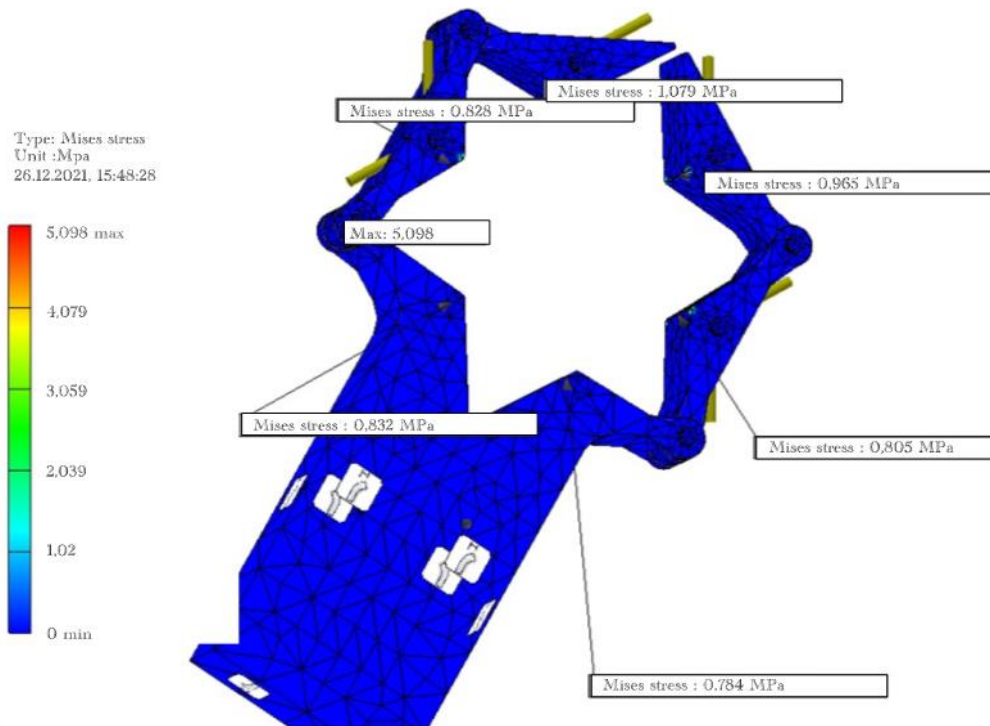
From Table 1 and Figure 2, it can be seen that if the object to be grasped requires an approximate force of 70 N at six points of contact with the gripper, then the force in drive-1 should be S1 = 100 n, and in drive-2 it should be S2 = 20n. These values for S1 and S2 were found by the method of fitting values.

Table 1 also shows an approximately linear relationship between the values of the rows in this table. It follows that if another, more or less, weak or strong compression is needed, then it is not difficult to find it by multiplying the found string of values by a normalizing factor, which is equal to the ratio of the desired compression to the found one.

### 3. Results

The flat model shows the general patterns of interconnection of the efforts of the "fingers" of the grip with the round object of the grip.

Let's consider a 3D model of this gripper. The calculated parameters of the 3D model are: metric parameters of a flat scheme, the thickness of the phalanges was taken to be the same for all phalanges and equal to 20 mm. In the computational model, the contact between the teeth and the cylinder in the form of a thin strip with dimensions of 20x2 mm was taken.



**Figure 5.**  
Von Mises stresses at the points of contact of the gripper.

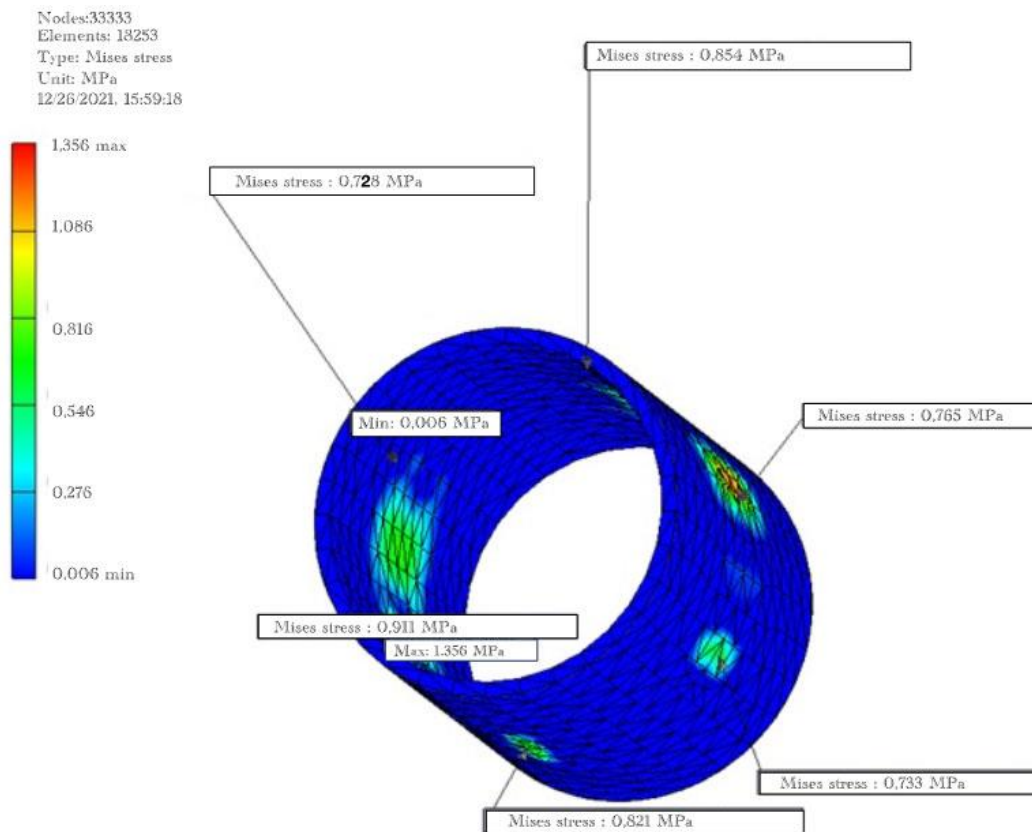


**Figure 6.**  
Von Mises stresses at the contact points of the seized object.

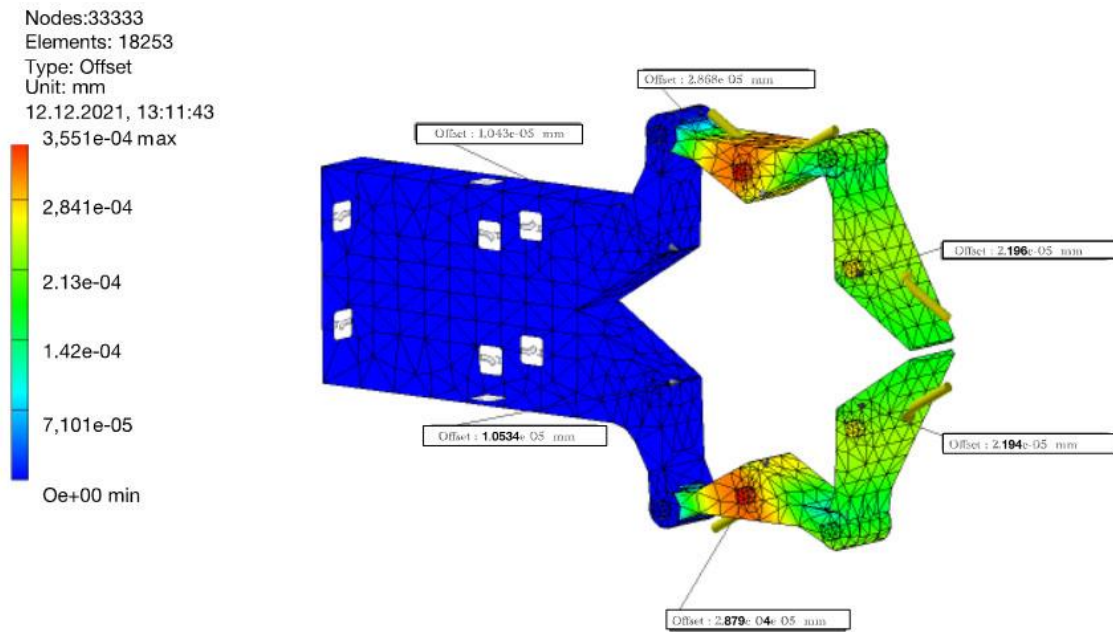


**Figure 7.**  
Elastic displacements at the points of contact of the gripper.

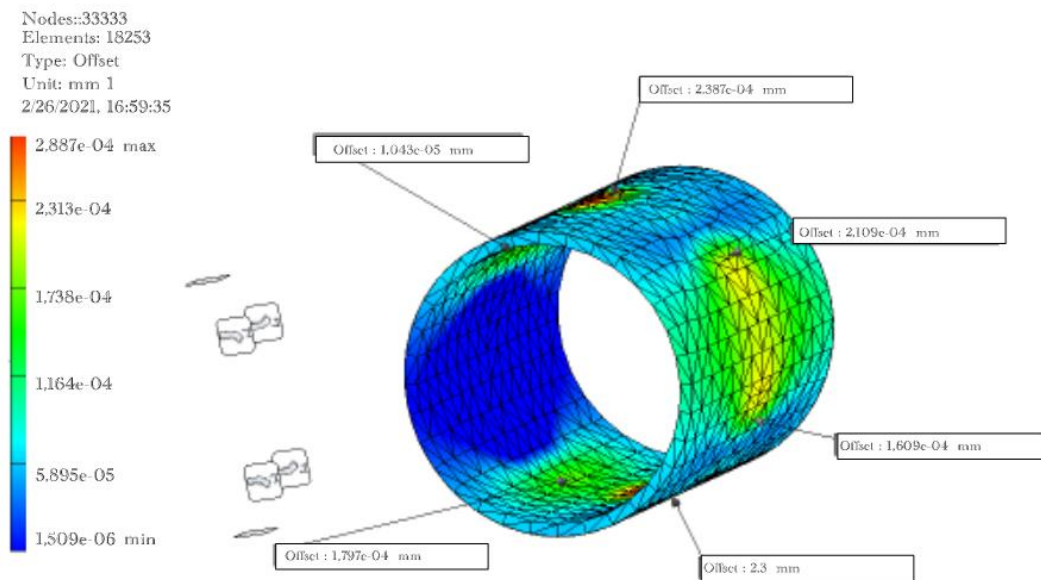


**Figure 8.**  
Elastic displacements at the points of contact of the object to be grasped.

Figures 5-8 show (on indicators) the values of stresses and elastic displacements at the points of the contact lines of the teeth of the 3D models of the gripper and the object to be seized. The picture of the efforts in a flat scheme and the von Mises stress values of 3D models show a certain similarity in the uniformity of the distribution of these parameters. On the left in Figures 3-6, there are color scales with the values of the corresponding parameters. The calculation was carried out by finite element modeling on Inventor.

#### 4. Conclusions and Discussion

From the analysis of the preferred selection points, we can conclude that the model behaves precisely and, in certain variants, strongly and strictly recreates the real physical system. The main advantage of using mechanical modeling to find capture points is that we can strictly establish a random abundance of object capture points with various parameter options. In addition, it is possible to simulate the difficult action of robotic grips along with alternatives to 2-F robotic grips (different width and depth of fingers, stroke span, etc.), because the model may be modified; however, in this case, a few changes to the initial model are necessary. The main disadvantage of the model is that for this type of modeling, clear contact values and settings of other parameters are required, which are not easy to test without actuating action or torque sensors. In addition, more time is needed to process the simulation because it strictly models the physics of the real world and does not make assumptions based on RGB-D data or point clouds.

The majority of scientific publications devoted to the study of grips mainly concern the issues of their structure, design, and control. Here, the grips are considered from the point of view of the criteria of adaptability and optimal distribution of forces in the grip. Flat schemes and 3D models of two-phalangeal, two-finger grips are considered. Their adaptability to the shape of a round cylinder or sphere is shown. The conditions under which an approximate uniform compression of an object occurs at six and eight points of contact of two-phalangeal grips with two fingers are shown. The practical significance of this approach is undeniable, since agricultural products (tomatoes, apricots, etc.) can be very sensitive even to minor deformations, and uniform nominal compression allows them to be reduced. In further studies, models for three parallel fingers will be made. In conclusion, adaptive gripping represents a promising achievement in the field of robotic finger design, providing a newfound path to solving problems connected with manual dexterity. Due to the wide range of capture systems and the complexity of the mechanism, it provides a basis for future studies of its probable applications and capabilities in numerous academic and industrial settings.

## References

- [1] Z. Ren, N. Kashiri, C. Zhou, and N. G. Tsagarakis, "Heri ii: A robust and flexible robotic hand based on modular finger design and under actuation principles," in *2018 IEEE/RSJ International Conference on Intelligent Robots and Systems (IROS)*, 2018: IEEE, pp. 1449-1455: <https://doi.org/10.1109/iros.2018.8594507>.
- [2] W. Ryu, Y. Choi, Y. J. Choi, and S. Lee, "Development of a lightweight prosthetic hand for patients with amputated fingers," *Applied Sciences*, vol. 10, no. 10, p. 3536, 2020. <https://doi.org/10.3390/app10103536>
- [3] M. Wahit, S. Ahmad, M. Marhaban, C. Wada, and L. Izhar, "3d printed robot hand structure using four-bar linkage mechanism for prosthetic application," *Sensors*, vol. 20, no. 15, pp. 1-22, 2020. <https://doi.org/10.3390/s20154174>
- [4] C. Wu, A. Song, H. Zhang, and C. Feng, "A backstepping control strategy for prosthetic hand based on fuzzy observation of stiffness," *Robot*, vol. 35, no. 6, pp. 686-691, 2013. <https://doi.org/10.3724/sp.j.1218.2013.00686>
- [5] L. Liow, A. B. Clark, and N. Rojas, "Olympic: A modular, tendon-driven prosthetic hand with novel finger and wrist coupling mechanisms," *IEEE Robotics and Automation Letters*, vol. 5, no. 2, pp. 299-306, 2019. <https://doi.org/10.1109/ra.2019.2956636>
- [6] D. N. O. Van and D. S. C. K. Van, "Functionality of i-LIMB and i-LIMB Pulse hands: Case report," *Journal of Rehabilitation Research and Development*, vol. 50, no. 8, p. 1123, 2013. <https://doi.org/10.1682/jrrd.2012.08.0140>
- [7] L. Dang, J. Song, Y. Wei, and W. Zhang, "COSA-LET finger: A novel coupled and self-adaptive robot finger with a linear empty-trip transmission," in *2017 2nd International Conference on Advanced Robotics and Mechatronics (ICARM)*, 2017: IEEE, pp. 334-338.
- [8] J. T. Belter, J. L. Segil, A. M. Dollar, and R. F. Weir, "Mechanical design and performance specifications of anthropomorphic prosthetic hands: A review," *The Journal of Rehabilitation Research and Development*, vol. 50, no. 5, p. 599, 2013. <https://doi.org/10.1682/jrrd.2011.10.0188>
- [9] T. Zhang, S. Fan, J. Zhao, L. Jiang, and H. Liu, "Design and control of a multisensory five-finger prosthetic hand," in *Proceeding of the 11th World Congress on Intelligent Control and Automation*, 2014: IEEE, pp. 3327-3332.
- [10] X.-L. Li, L.-C. Wu, and T.-Y. Lan, "A 3D-printed robot hand with three linkage-driven underactuated fingers," *International Journal of Automation and Computing*, vol. 15, pp. 593-602, 2018. <https://doi.org/10.1007/s11633-018-1125-z>
- [11] C.-H. Liu *et al.*, "Optimal design of a soft robotic gripper for grasping unknown objects," *Soft Robotics*, vol. 5, no. 4, pp. 452-465, 2018. <https://doi.org/10.1089/soro.2017.0121>
- [12] M. F. Reis, A. C. Leite, and F. Lizaralde, "Modeling and control of a multifingered robot hand for object grasping and manipulation tasks," in *2015 54th IEEE Conference on Decision and Control (CDC)*, 2015: IEEE, pp. 159-164.
- [13] P. Wattanasiri, P. Tangpornprasert, and C. Virulsri, "Design of multi-grip patterns prosthetic hand with single actuator," *IEEE Transactions on Neural Systems and Rehabilitation Engineering*, vol. 26, no. 6, pp. 1188-1198, 2018. <https://doi.org/10.1109/tnsre.2018.2829152>
- [14] F. Cordella *et al.*, "A force-and-slippage control strategy for a poliarticulated prosthetic hand," in *2016 IEEE International Conference on Robotics and Automation (ICRA)*, 2016: IEEE, pp. 3524-3529.
- [15] G. Palli *et al.*, "The DEXMART hand: Mechatronic design and experimental evaluation of synergy-based control for human-like grasping," *The International Journal of Robotics Research*, vol. 33, no. 5, pp. 799-824, 2014. <https://doi.org/10.1177/0278364913519897>
- [16] C. Wu *et al.*, "Mechanical-sensor integrated finger for prosthetic hand," in *2018 IEEE International Conference on Robotics and Biomimetics (ROBIO)*, 2018: IEEE, pp. 1465-1470.
- [17] J. Venter and A. M. Mazid, "Tactile sensor based intelligent grasping system," in *2017 IEEE International Conference on Mechatronics (ICM)*, 2017: IEEE, pp. 303-308.
- [18] E. Luberto, Y. Wu, G. Santaera, M. Gabiccini, and A. Bicchi, "Enhancing adaptive grasping through a simple sensor-based reflex mechanism," *IEEE Robotics and Automation Letters*, vol. 2, no. 3, pp. 1664-1671, 2017. <https://doi.org/10.1109/ra.2017.2681122>
- [19] W. Park, K. Ro, S. Kim, and J. Bae, "A soft sensor-based three-dimensional (3-D) finger motion measurement system," *Sensors*, vol. 17, no. 2, p. 420, 2017. <https://doi.org/10.3390/s17020420>
- [20] A. Othman, N. Hamzah, Z. Hussain, R. Baharudin, A. D. Rosli, and A. I. C. Ani, "Design and development of an adjustable angle sensor based on rotary potentiometer for measuring finger flexion," presented at the 2016 6th IEEE International Conference on Control System, Computing and Engineering (ICCSCE), 2016.
- [21] U. A. Hofmann, T. Bützer, O. Lamberg, and R. Gassert, "Design and evaluation of a bowden-cable-based remote actuation system for wearable robotics," *IEEE Robotics and Automation Letters*, vol. 3, no. 3, pp. 2101-2108, 2018. <https://doi.org/10.1109/ra.2018.2809625>
- [22] U. Jeong and K.-J. Cho, "A feasibility study on tension control of Bowden-cable based on a dual-wire scheme," in *2017 IEEE International Conference on Robotics and Automation (ICRA)*, 2017: IEEE, pp. 3690-3695.
- [23] J. L. Brito, M. X. Quinde, D. Cusco, and J. I. Calle, "Study of the state of the art of hand prostheses," *Ingenius. Revista De Ciencia y Tecnología*, no. 9, pp. 57-64, 2013. <https://doi.org/10.17163/ings.n9.2013.08>

- [24] B. Peerdeman *et al.*, "Myoelectric forearm prostheses: State of the art from a user-centered perspective," *Journal of Rehabilitation Research & Development*, vol. 48, no. 6, pp. 719–738, 2011. <https://doi.org/10.1682/jrrd.2010.08.0161>
- [25] C. Piazza *et al.*, "The soffthand pro-h: A hybrid body-controlled, electrically powered hand prosthesis for daily living and working," *IEEE Robotics & Automation Magazine*, vol. 24, no. 4, pp. 87-101, 2017. <https://doi.org/10.1109/mra.2017.2751662>
- [26] G. Smit, R. M. Bongers, C. K. Van der Sluis, and D. H. Plettenburg, "Efficiency of voluntary opening hand and hook prosthetic devices: 24 years of development?," *Journal of Rehabilitation Research and Development*, vol. 49, no. 4, pp. 523-534, 2012. <https://doi.org/10.1682/jrrd.2011.07.0125>
- [27] D. Datta, K. Selvarajah, and N. Davey, "Functional outcome of patients with proximal upper limb deficiency–acquired and congenital," *Clinical Rehabilitation*, vol. 18, no. 2, pp. 172-177, 2004. <https://doi.org/10.1191/0269215504cr716oa>
- [28] D. J. Atkins, D. C. Heard, and W. H. Donovan, "Epidemiologic overview of individuals with upper-limb loss and their reported research priorities," *Jpo: Journal of Prosthetics and Orthotics*, vol. 8, no. 1, pp. 2-11, 1996. <https://doi.org/10.1097/00008526-199600810-00003>
- [29] A. Singh, "Prosthetic hand control," *International Journal of Engineering Research and Applications*, vol. 2, no. 6, pp. 311-339, 2012.
- [30] G. J. Pollayil, M. J. Pollayil, M. G. Catalano, A. Bicchi, and G. Grioli, "Sequential contact-based adaptive grasping for robotic hands," *The International Journal of Robotics Research*, vol. 41, no. 5, pp. 543-570, 2022. <https://doi.org/10.1177/02783649221081154>
- [31] I. Hussain *et al.*, "Compliant gripper design, prototyping, and modeling using screw theory formulation," *The International Journal of Robotics Research*, vol. 40, no. 1, pp. 55-71, 2021. <https://doi.org/10.1177/0278364920947818>
- [32] D. Ji, J. Lee, and M. Jin, "Design and control of hybrid Flexible robotic gripper with high stiffness and stability," presented at the 2022 13th Asian Control Conference (ASCC), 2022.
- [33] I. Hashira, R. Kato, and K. Ishizaka, "Development of a humanoid hand system to support robotic urological surgery," in *2022 44th Annual International Conference of the IEEE Engineering in Medicine & Biology Society (EMBC)*, 2022: IEEE, pp. 4849-4852.
- [34] P. Bencak, D. Hercog, and T. Lerher, "Simulation model for robotic pick-point evaluation for 2-F robotic Gripper," *Applied Sciences*, vol. 13, no. 4, p. 2599, 2023. <https://doi.org/10.3390/app13042599>